Available online at www.sciencedirect.com
ScienceDirect
Journal of Solid State Chemistry 180 (2007) 3325–3332
JOURNAL OF SOLID STATE CHEMISTRY
www.elsevier.com/locate/jssc

Irradiation-induced reduction and luminescence properties of Sm^{2+} doped in $BaBPO_5$

Yanlin Huang[a], Kiwan Jang[b,*], Wanxue Zhao[a], Eunjin Cho[b], Ho Sueb Lee[b], Xigang Wang[a], Dake Qin[a], Ying Zhang[a], Chanfang Jiang[a], Hyo Jin Seo[c]

[a]*School of Material Engineering, Soochow University, 178 GanJiang East Road, Suzhou 215021, PR China*
[b]*Department of Physics, Changwon National University, Changwon 641-773, Republic of Korea*
[c]*Department of Physics, Pukyong National University, Daeyeon 3-Dong 599-1, Pusan 608-737, Republic of Korea*

Received 6 July 2007; received in revised form 18 September 2007; accepted 21 September 2007
Available online 2 October 2007

Abstract

Usually, Sm^{2+} ions could be reduced by heating the materials in reducing atmospheres. Exposure to ionizing radiations is also known to cause $Sm^{3+} \rightarrow Sm^{2+}$ conversion. In this work, $BaBPO_5$ doped with the samarium ion was prepared by high temperature solid-state reaction. Sm^{2+} ions were obtained by two different reduction methods, i.e., heating in H_2 reduced atmosphere and X-ray irradiation. The measurements of X-ray diffraction (XRD), and scanning electron microscope (SEM) were investigated. It is found that the conversion of $Sm^{3+} \rightarrow Sm^{2+}$ is very efficient in $BaBPO_5$ hosts after X-ray irradiation. Sm^{2+} ions under these two reduction methods exhibit different characteristics that were studied by measurements of luminescence and decay. The results showed that the luminescence properties of Sm^{2+} ions in $BaBPO_5$ were highly dependent on the sample preparation conditions.

PACS: 81.40.Wx; 81.10.Jt; 78.55.Hx; 61.80.Cb

Keywords: X-ray irradiation; Borophosphates; Luminescence; Sm^{2+}; Reduction

1. Introduction

Over the past years, Rare-earth-activated inorganic materials, e.g., borates, phosphates and borophosphates, have long been established as useful luminescent materials in fabricating the optoelectronic devices. Nowadays, more and more interest has been focused on the synthesis and photoluminescence of new rare earth compounds due to their potential applications [1–7]. And there have been many interests in research of Sm^{2+} doped materials since persistent spectral hole burning (PSHB) at room temperature (RT) was reported in Sm^{2+} doped fluoride single crystals [8]. The Sm^{2+} ions doped inorganic materials can show relatively high thermal stability [9], and have been widely investigated because of their potential use in frequency domain optical storage [10–12].

Usually, Sm ions are stable in their trivalent state in many host materials. So it is necessary to reduce the Sm^{3+} ions to Sm^{2+} ions before the application of luminescence Sm^{2+} ions is explored. The very common method is heating the materials under reducing atmosphere. The second method for the reduction of Sm^{2+} is to irradiate by X-ray irradiation [13,14], or high intensity laser irradiation, such as femto-second laser pulses [15].

However, it was also reported that the Sm^{3+} ions could be reduced to Sm^{2+} when the certain hosts materials were prepared in air, such as BaB_8O_{13}, SrB_6O_{10} and SrB_4O_7 [16–18]. The stabilization of Sm^{2+} in such kind of material is because of its unique structure. For an example, in SrB_4O_7, all of the boron atoms are tetrahedrally coordinated to form a three-dimensional $(B_4O_7)_\infty$ network by corner sharing. The network contains channels parallel to *b*-axis. The strontium ions fit into these channels and are

*Corresponding author. Fax: +82 55 267 0264.
E-mail addresses: huangyanlin@hotmail.com (Y. Huang), kwjang@changwon.ac.kr (K. Jang).

0022-4596/$ - see front matter © 2007 Elsevier Inc. All rights reserved.
doi:10.1016/j.jssc.2007.09.030

surrounded by nine oxygen ions, giving SrO_9 polyhedral. The divalent rare earth ions are thus located in a "cage" formed by BO_4 units of the $(B_4O_7)_\infty$ framework. Such a framework is thought to be a rigid structure preventing the divalent rare-earth ions from being oxidized [16]. Taking into consideration of this suggestion of a necessary rigid structure to stable the Sm^{2+} ions, borophosphates are expected to be a good candidate, because the structure of these borophosphates also has some similar characteristics to what mentioned above, and boron and phosphorous can also form rigid BO_4 and PO_4 units in this host.

Borophosphates constitute a class of compounds. In the $SrO–B_2O_3–P_2O_5$ system, for an example, the crystalline alkaline earth borophosphates $MBPO_5$ ($M = Ca^{2+}$, Sr^{2+}, Ba^{2+}) were reported to be isostructural with stillwellite-$LnBSiO_5$ (Ln refers to lanthanide), built up by BO_4 and SiO_4 tetrahedron [19]. Each BO_4 tetrahedron is connected with two SiO_4 tetrahedron and has two common edges with the lanthanide polyhedra of adjacent columns forming helical chains. Lanthanide ions are located in the center of this helix and coordinated with nine oxygens as LnO_9 polyhedral. This structure also suggests that the hosts $MBPO_5$ should be a good candidate for the divalent rare-earth ions [20–22].

The compound $BaBPO_5$ was first reported by Bauer [23]. It was also confirmed to be an incongruently melting compound by the investigation on the sub-solid phase relations in the ternary system $BaO–B_2O_3–P_2O_5$ [24]. Attentions have been paid to the luminescence of rare earth in $MBPO_5$ hosts. Blasse [25] has reported the UV excited blue emission of $MBPO_5:Eu^{2+}$ ($M = Ca^{2+}$, Sr^{2+}, Ba^{2+}) prepared in H_2/N_2 reducing atmosphere. Large crystals of $BaBPO_5$ have been obtained with the improvement of growth method [26]. Qinghua Zeng et al. [19] has prepared the Sm^{2+} ions doped $BaBPO_5$ in reduced atmosphere of H_2/He (20% H_2). They studied temperature dependences of the luminescence and lifetime of $^5D_0 \rightarrow {}^7F_0$ transition in Sm^{2+} ions.

In this study, the Sm^{2+}-doped $BaBPO_5$ crystals were prepared by two different reduction methods, i.e., thermal treatment in reduced atmosphere and X-ray irradiation of the sample as-made in air. XRD and IR spectra were analyzed for these samples. The luminescence spectra and decay curves from Sm^{2+} ions were detected under excitation of 488 Ar^+ ions laser and 532 nm pulsed laser, respectively.

2. Experiments

The Sm^{3+} and Sm^{2+} doped $BaBPO_5$ (BBP) were prepared by solid-state reactions in air and a reduction atmosphere, respectively. Stoichiometric amounts of reagent grade $BaCO_3$, H_3BO_3 (3 mol% excess to compensate for the BO_3 evaporation), $(NH_4)_2HPO_4$ were thoroughly mixed and ground. The mixtures were heated at 500 °C. The obtained powder and 0.5 mol% Sm_2O_3 were thoroughly mixed by grinding together and then heated secondly up to 950 °C for 8 h in air and in a reduction atmosphere ($N_2/H_2 = 95:5$), respectively. After that $BaBPO_5:Sm^{3+}$ sample prepared in air was irradiated with X-ray for 10 h using Cu$K\alpha$ line (45 kV and 300 mA). That is to say, we have two methods to reduce the Sm^{2+} ions. The sample heated in reduced atmosphere of H_2 were denoted as BBP-H; and the sample prepared in air and then irradiated by X-ray was denoted as BBP-X.

Powder X-ray diffraction (XRD) data were collected at RT on a Rigaku D/Max diffractometer operating at 40 kV, 30 mA using Cu$K\alpha$ radiation. The morphological features of the BBP samples were investigated by scanning electron microscope (JEOL, SEM).

Divalent Sm^{2+} ion has the $4f^6$ electron configuration, which under irradiation with UV and visible light can be excited into the $4f^55d^1$ continuum. The excitation of divalent samarium takes place via the strong $4f^55d^1$ bands from which the ions quickly decay to the lower metastable level. To measure the emission spectra of samarium ions (Sm^{2+} and Sm^{3+}), the samples were excited by using the 488-nm line of an argon-ion laser and the luminescence was then detected with a photomultiplier tube (PMT, Hamamatsu, R928) mounted on a spectrometer (Dongwoo, DM701) for high-resolution spectra. For the low temperature luminescence measurements, the samples were placed in a liquid helium flow cryostat in the variable-temperature region (10–300 K). The low-resolution spectra were performed on a fiber optic spectrometer (PC 2000, Ocean Optics). An OG-530 cut-off filter was placed in front of the spectrometer to block off the scattered laser lines. The luminescence decay were measured by a pulsed yttrium aluminum garnet (Nd:YAG) laser (Spectron Laser Sys. SL802G).

3. Results and discussion

The SEM pictures of $BaBPO_5:Sm^{3+}$ powders sintered at 950 °C are shown in Fig. 1. The grains have a uniform shape of ball particles with an average size of about 0.5–1 μm. This shows that the solid reactions of the mixtures took place well. Then, the structure was checked by FT-IR and X-ray powder diffraction. The XRD results shown in Fig. 2 indicated that all samples were single hexagonal phases, which were in good agreement with those given in JCPDS 19–96. The diffraction peaks of the powders are indexed as $BaBPO_5$ phase and no impurity peaks were observed.

Photoluminescence was used to determine the valence state of the Sm ions. The low-resolution photoluminescence spectra at RT in the range from 500 to 850 nm were obtained using 488 nm Ar^+-ion laser. Fig. 3 shows the emission spectra of $BBP:Sm^{3+}$ heated in air and that subsequentially irradiated by X-ray (BBP-X). The sample as-prepared in air contains only Sm^{3+} ions and shows fluorescence bands at 563, 598, 644 and 703 nm which are due to the $^4G_{5/2}$ to $^6H_{5/2}$, $^6H_{7/2}$, $^6H_{9/2}$, and $^6H_{11/2}$ transitions from the Sm^{3+} ion, respectively (Fig. 3a),

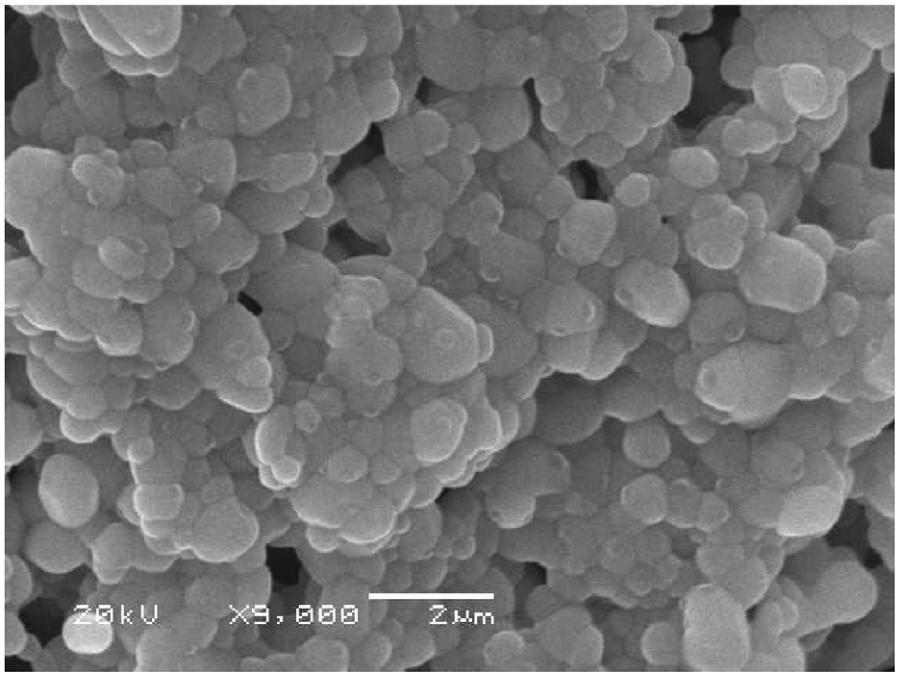

Fig. 1. The SEM pictures for the Sm doped $BaBPO_5$ powders.

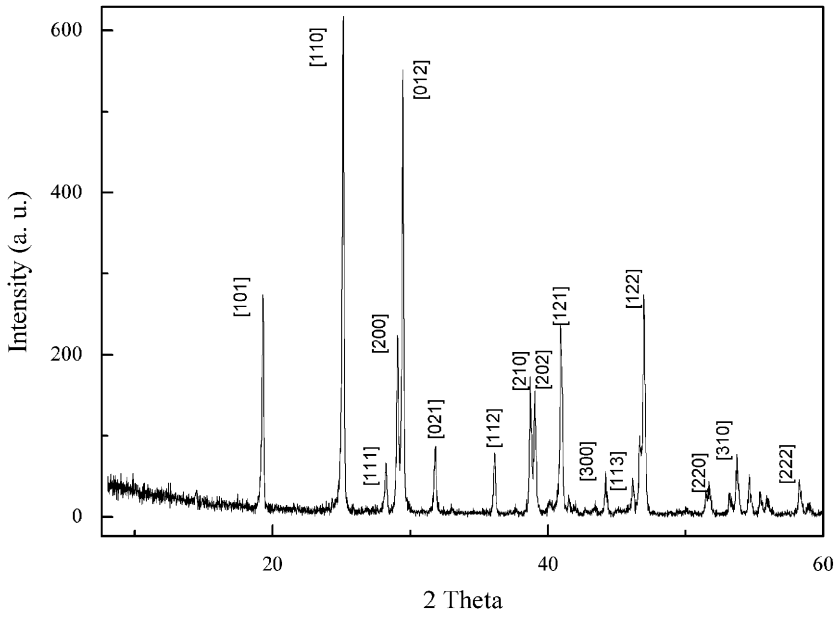

Fig. 2. The X-ray diffraction patterns of the $BaBPO_5$ powders.

indicating that this ion was not reduced". On the other hand, several groups of sharp lines are observed in the emission spectra of the BBP-X sample, which is mainly due to the Sm^{2+} transitions between the energy levels of $4f^6$ electronic configurations (Fig. 3b). Even by enlarging the spectra between 500 and 700 nm, no any emission from the Sm^{3+} ions could be found. This means that the Sm^{3+} ions were all successfully reduced to Sm^{2+} ions during the X-ray irradiation process.

Fig. 4 shows the high-resolution emission spectra of BBP-X recorded at RT using the excitation wavelength of 488 nm laser. It presents several groups of narrow lines whose lines are centered at about 680, 689, 691 and 705 nm from Sm^{2+} ions. The strongest fluorescent peak (680 nm) in these spectra is from the $^5D_0 \rightarrow {}^7F_0$ transition of Sm^{2+} and other groups were assigned to $^5D_0 \rightarrow {}^7F_1$ transitions of Sm^{2+} ions. In Fig. 4, some additional lines situated at the lower energy side of the $^5D_0 \rightarrow {}^7F_0$, and $^5D_0 \rightarrow {}^7F_1$ transitions could be observed. They are ascribed to the vibronic transitions, resulting from the interactions between the electrons and the lattice during the transitions between these two levels. The energy displacement with

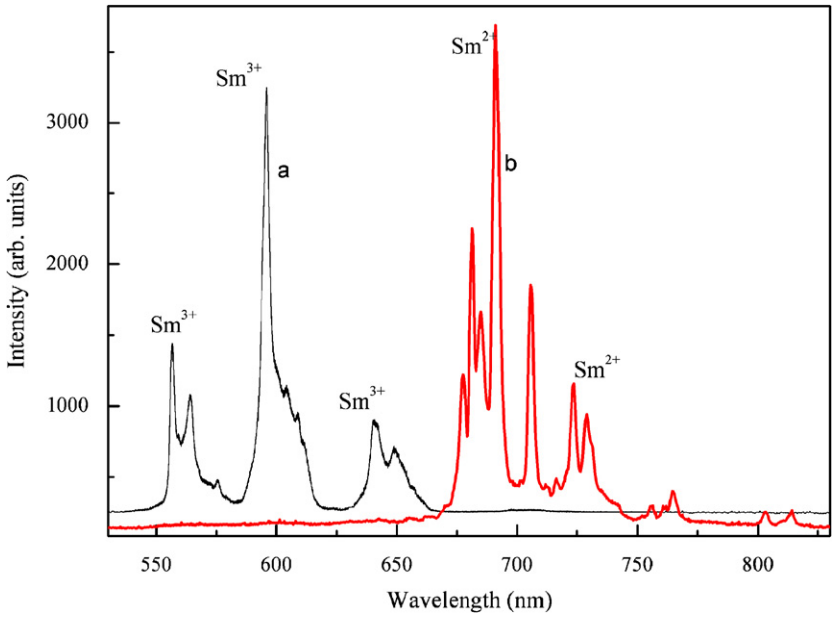

Fig. 3. The RT low-resolution emission of Sm-doped $BaBPO_5$ sample prepared in air atmosphere. The excitation is 488 nm laser. (a) The as-made sample; (b) the as-made sample after X-ray irradiation.

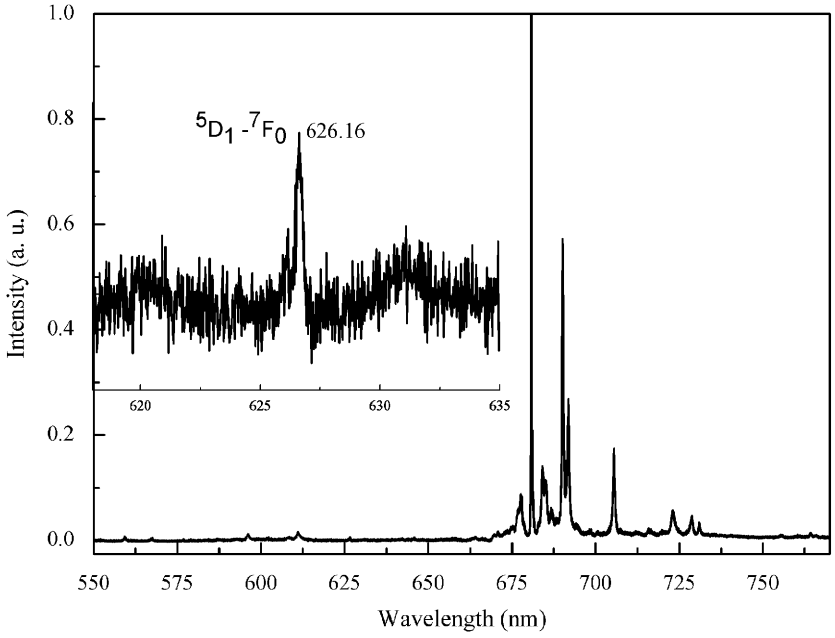

Fig. 4. The high-resolution emission spectra of Sm^{2+} in BBP-X recorded at RT using the excitation wavelength of 488 nm laser. The enlargement of the spectrum in the insert shows the $^5D_1 \rightarrow {}^7F_0$ transition.

zero-phonon line (ZPL) is at 68 and 128 cm^{-1} in each side of $^5D_0 \rightarrow {}^7F_0$ and $^5D_0 \rightarrow {}^7F_1$ transitions, respectively. Their intensities increase with increasing temperature. At lower temperature, all these vibronic transitions were disappeared.

In the BBP-X, at lower temperature below 200 K, no emission lines due to the transitions between $^5D_1 \rightarrow {}^7F_J$ were observed. However, it was detected at RT in Fig. 4, where the enlargement of the spectrum in the inset shows the $^5D_1 \rightarrow {}^7F_0$ transition at 626.1 nm; Its intensity increases when the temperature is enhanced, as it results from the $^5D_1$ level due to the excited electrons in the $^5D_1$ rapidly relax into the $^5D_0$ level nonradiatively by thermal interaction with lattices [27]. The same phenomena were also observed in Sm doped BBP prepared in H_2 reduced atmospheres [19].

Fig. 5 shows the comparison of the high-resolution emission spectra of Sm^{2+} doped in BBP-H and BBP-X. The spectra were recorded at 10 K using the excitation wavelength of 488 nm laser. The emission of Sm^{2+} in the

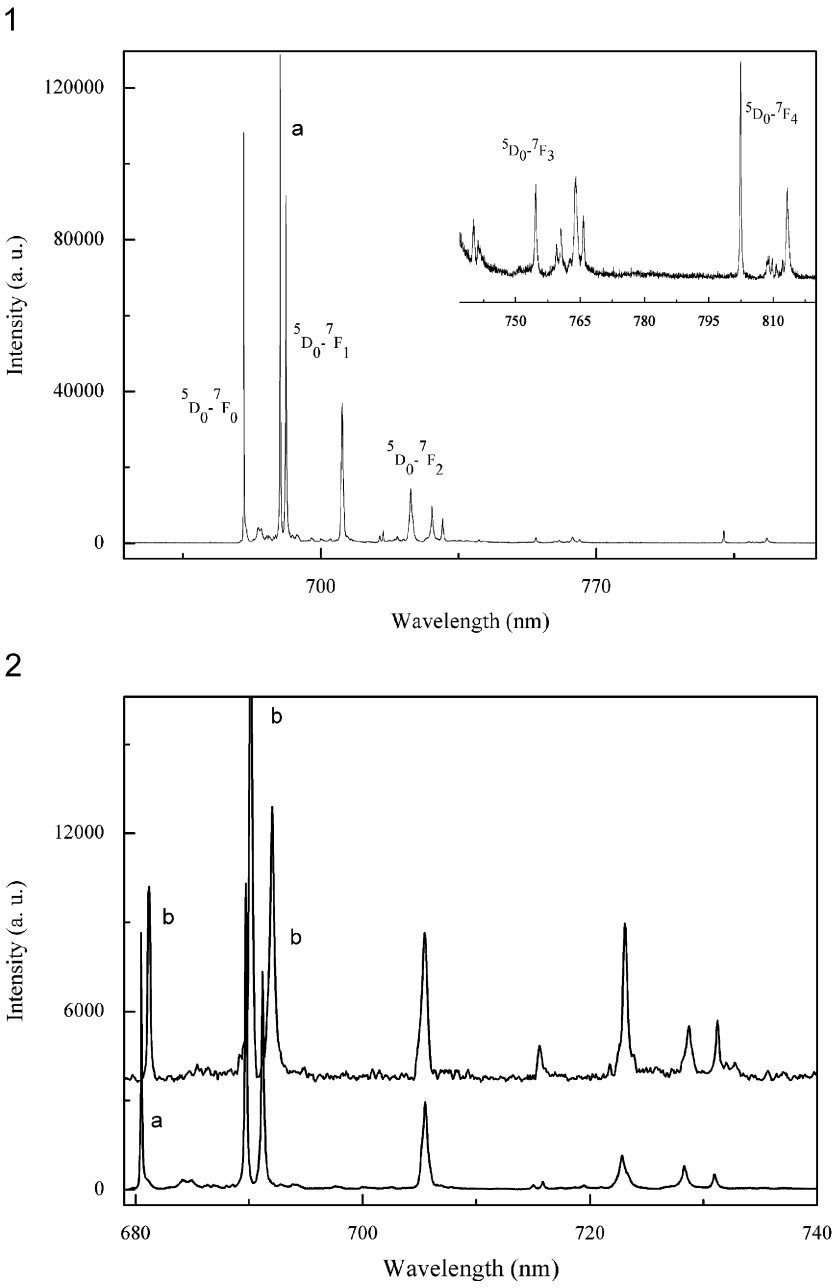

Fig. 5. The high-resolution emission spectra of Sm^{2+} in BBP-X (1); and the comparison with that of BBP-H (2). BBP-X; (a) and the comparison with that of BBP-H ; (b) the spectra were recorded at 10 K using the excitation wavelength of 488 nm laser.

two materials shows similar features and results from transitions between levels of the $4f^6$ electron configuration. The emission related to the Sm^{3+} ions between 500 and 670 nm can be hardly detected. The result of the $^5D_0 \rightarrow {}^7F_J$ transitions and their assignments are listed in Table 1, and were compared with the results obtained in [19].

In BBP-X and BBP-H, there is only one line for the $^5D_0 \rightarrow {}^7F_0$ transition, three for the $^5D_0 \rightarrow {}^7F_1$ transitions, and five for $^5D_0 \rightarrow {}^7F_2$ transition. This is in agreement with the theoretical splitting of the ^7F_J ($J = 0$, 1, 2) multiplet into a maximum of one, three and five sublevels for the corresponding levels. The intensity ratio of $^5D_0 \rightarrow {}^7F_1$ emission to $^5D_0 \rightarrow {}^7F_0$ emission increased when the temperature get down. Roughly speaking, it means that local field symmetry around Sm^{2+} ions increased at lower temperature, because the $^5D_0 \rightarrow {}^7F_0$ transition probability decreases sensitively with an increase of the environmental symmetry, while the $^5D_0 \rightarrow {}^7F_1$ transition probability is approximately constant [28].

The luminescence lifetimes of the $^5D_0 \rightarrow {}^7F_0$ transition in SBP were recorded at RT under pulsed 532 nm laser. The decay curves in BBP-H exhibit an exact single exponential with a lifetime of 8.16 ms at 300 K (Fig. 6a), but that of Sm^{2+} created by X-ray irradiation in BBP-X does not exhibit an exact single exponential. As shown in Fig. 6b, because the phosphorescence decay could be due to a sum

of several first-order decays related to the emptying of several different traps, The decay curve has been analyzed by curve fitting and found that it can be fitted perfectly using the bi-exponential decay function

$$I = A_1 \exp(-t/\tau_1) + A_2 \exp(-t/\tau_2), \quad (1)$$

where I is the phosphorescence intensity at time t; A_1 and A_2 are constants; τ_1 and τ_2 are the decay times. The fitting parameters obtained are:$\tau_1 = 0.47$ ms and $\tau_2 = 7.025$ ms.

The population decay in the initial stage in Fig. 6b with a very short lifetime of $\tau_1 = 0.47$ ms indicates there are some energy transfer occurred under this excitation at RT. The reason is not clear here. But this should be related to the energy transfer among Sm ions or with some defects in the lattices.

Note that, in BBP crystal especially the X-ray irradiated samples, there are many possible defects, which maybe due to the intrinsic factors or extrinsic effects of RE doping. The action of X-ray irradiation is to produce secondary electrons from the sites where they are in a stable state and have excess energy. Such electrons may traverse in the lattice depending upon their energy and the composition and are finally be trapped. The trapping sites may be the lattices ions, the structural defects due to impurities and intrinsic defects.

W. Li et al. [29] have found that X-ray excited luminescence of BBP have a broad luminescence band extends from 300 to 550 nm correspond to different transition mechanisms due to defects of the BBP matrix. After X-ray irradiation, $BaBPO_5$ crystal shows four induced absorption centered at about 304, 418, 580 and 740 nm, respectively. This indicates the presence of some trapping sites in the crystal and some local defect energy levels are formed in the energy band gap. This might be created by inevitable non-equal evaporation during preparation and thus results in the formation of intrinsic defects, such as cation and oxygen vacancies. Positional

Table 1
The assignments and the peak positions of the Sm^{2+} emission band at 10 K in BBP-X and BBP-H shown in Fig. 5, which is compared with that of Sm^{2+} ions in $BaBPO_5$ at 77 K in [19]

$^5D_0 \rightarrow {}^7F_J$	BBP-X	BBP-H	$BaBPO_5$:Sm^{2+} in [19]
$J = 0$	680.496	681.23	681.1
$J = 1$	689.712	690.25	690.5
	691.205	692.025	692.0
	705.528	705.45	705.7
$J = 2$	715.032	715.575	715.9
	715.848	716.025	716.1
	722.856	723.075	723.2
	728.28	728.70	728.8
	730.968	731.25	731.1
$J = 3$	740.136		
	741.24		
	754.776		
	759.576		
	760.448		
	764.016		
	765.744		
$J = 4$	802.441		
	808.584		
	809.064		
	809.789		
	810.768		
	812.232		
	813.264		

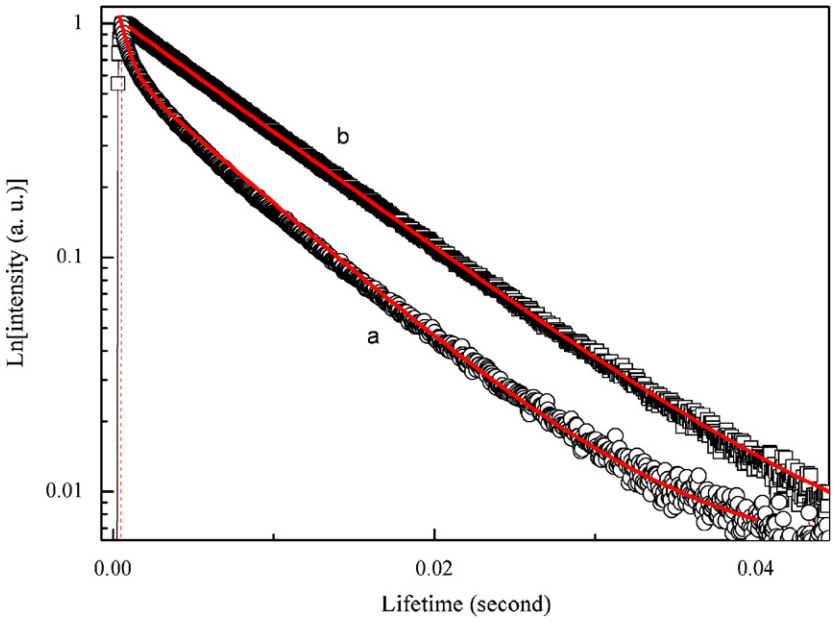

Fig. 6. The decay profiles of the $^5D_0$ fluorescence at 10 K under $^5D_0 \rightarrow {}^7F_0$ transition by exciting at pulsed laser 532 nm for (a) prepared in air after X-ray irradiation; (b) Prepared in H_2 atmosphere.

disorder of B and vacant B (V'''_B) have been reported in $SrBPO_5$ crystal on the basis of thermal displacement parameters for B and XPS data [30]. In BBP, B^{3+} and P^{5+} ions have so may similarity chemical characteristics, for examples, the approximate electro-negaitivity (2.04 for B, 2.19 for P), close ionic radius (0.11 nm for B^{3+}, 0.17 nm for P^{5+}) [31] and the same coordinating environment (both are coordinated by 4 oxygen atoms), the creation of antisite defects, B-site P^{5+} ion $(P_B)^{\bullet\bullet}$, is also possible. In the BBP lattice, trivalent Sm^{3+} occupies the lattice of divalent Ba^{2+} and thus two Sm^{3+} should be needed to substitute three Ba^{2+} ions in order to maintain the charge balance. Hence, a vacancy defect, which will be negatively charged, is formed at the Ba^{2+} site. In a word, there exist rich defects in as-grown $BaBPO_5$. From the point of energy band theory, these defects will create defect energy levels in the band gap. It can be suggested that the electrons and holes introduced by X-ray excitation in the host might be mobile and lead to transition among conduction band, acceptor levels, donor levels and valence band [29].

In BBP-H and BBP-X, Sm^{2+} shows only a single emission line observed for the $^5D_0 \rightarrow {}^7F_0$ transition, revealing that only one crystallographic cationic site is available for Sm^{2+} in all the hosts. However, the positions of $^5D_0 \rightarrow {}^7F_0$ transition are different; they are 680.496 nm (14,695 cm^{-1}) and 681.23 nm (14,679 cm^{-1}) for BBP-X and BBP-H, respectively. And they have different luminescence delay behavior in Fig. 6. This indicates that local structure around the Sm^{2+} ions is different. And the defects might be different in these samples. Actually, usually in some oxide host, the reduction mechanism of Sm^{2+} by heating the materials in reduced atmosphere and X-ray irradiation are different [14].

In BBP-H, the Sm ions were doped in $BaBPO_5$ matrix as Sm^{2+} states during the sample preparation process. The Sm^{2+} ions in BBP-H are more chemically stable compared to those in BBP-X produced by X-ray irradiation. In Sm doped $BaBPO_5$ as-prepared in air, the Sm ions were doped in $BaBPO_5$ lattices in 3+ valence states initially. When trivalent Sm^{3+} occupies the lattice of divalent Ba^{2+}, two Sm^{3+} ions should be needed to substitute three Ba^{2+} ions in order to maintain the charge balance and thus resulting in the formation of vacancy defect negatively charged at the Ba^{2+} site. This vacancy defect having two negative charges can be become the donor of electrons, while the two Sm^{3+} become acceptors of electrons. Since the X-rays have high enough energy to excite the electrons in the donor level into the acceptor level, electrons of donor level can be transferred to the Sm^{3+} site by X-ray irradiation resulting in the reduction of Sm^{3+} to Sm^{2+}. Recently, Kiwan Jang et al. [13] have explained this kind of X-ray induced reduction mechanism in Sm^{3+} doped SrB_6O_{10}. The defects produced by X-ray irradiation are closely related with the excited Sm^{2+} ions, which are different from those created by heating in H_2 atmosphere. Consequentially, they have different luminescence.

Regrettably, to elucidate the detailed defects are difficult at present. To explain the X-ray induced reduction mechanism clearly, the detailed experiments including photo bleaching effects of Sm^{2+} by laser irradiation, induced absorption and thermoluminescence of BBP matrix under X-ray, and the other experiments were inquired.

4. Conclusion

The Sm^{3+} and (BBP) were prepared by solid-state reactions in air and a reduction atmosphere, respectively. The samarium ions in $BaBPO_5$ prepared in reduced atmosphere were doped into Sm^{2+} ions. In $BaBPO_5$ as-prepared in air, the Sm ions were doped in the lattices in Sm^{3+}, which can be efficiently convert to Sm^{2+} ions after X-ray irradiation. It is found that the conversion of $Sm^{3+} \rightarrow Sm^{2+}$ is very efficient in $BaBPO_5$ hosts after X-ray irradiation. $BaBPO_5$ is a suitable host for studying $Sm^{3+} \rightarrow Sm^{2+}$ conversion, and are a good candidate to accommodate Sm^{2+} ions. In BBP-H and BBP-X, Sm^{2+} ions show only a single emission line observed for the $^5D_0 \rightarrow {}^7F_0$ transition, revealing that only one crystallographic cationic site is available. However, the two samples show different local structures and different luminescence delay behavior. The luminescence decay curves of Sm^{2+} are single exponential in BBP-H with a lifetime of 8.16 ms. While, that of Sm^{2+} in BBP-X exhibit population decay in the initial stage with a short lifetime of 0.47 ms, followed by a decay of 7.025 ms. These differences in luminescence behavior are due to different defects created in the two reduction methods. In $BaBPO_5$, luminescence of Sm^{2+} ions was highly dependent on the sample preparation conditions.

Acknowledgments

This work was financially supported by Jiangsu Provincial Natural Science Foundation of China (BK-2007053), and the Second Stage of Brain Korea 21 Project (BK21) Corporations at Changwon National University.

References

[1] B. Moine, G. Bizarri, Opt. Mater. 28 (2006) 58.
[2] Xiaoyan Bai, Guochun Zhang, Peizhen Fu, J. Solid State Chem. 180 (2007) 1792.
[3] A.A. Babaryk, I.V. Zatovsky, V.N. Baumer, N.S. Slobodyanik, P.G. Nagorny, O.V. Shishkin, J. Solid State Chem. 180 (2007) 1990.
[4] K. Popa, D. Bregiroux, Rudy J.M. Konings, T. Gouder, A.F. Popa, T. Geisler, P.E. Raison, J. Solid State Chem. 180 (2007) 2346.
[5] L.N. Ji, H.W. Ma, J.B. Li, J.K. Liang, B.J. Sun, Y.H. Liu, J.Y. Zhang, G.H. Rao, J. Solid State Chem. 180 (2007) 2256.
[6] Xiaoyan Bai, Guochun Zhang, Peizhen Fu, J. Solid State Chem. 180 (2007) 1792.
[7] A. Haberer, G. Heymann, H. Huppertz, J. Solid State Chem. 180 (2007) 1595.
[8] R. Jaaniso, H. Bill, Europhys. Lett. 16 (1991) 569.

[9] P. Mikhail, M. Schnieper, H. Bill, J. Hulliger, Phys. Stat. Sol. B 215 (1999) R17.
[10] M. Nogami, K. Suzuki, Adv. Mater. 14 (2002) 923.
[11] M. Nogami, T. Hayakawa, Phys. Rev. B 56 (1997) 235.
[12] J. Qiu, K. Miura, K. Nouchi, T. Suzuki, K. Kondo, T. Mitsuyu, K. Hirao, Solid State Commun. 113 (2000) 341.
[13] K. Jang, Ilgon. Kim, Seongtae. Park, Y. Huang, H. Jin Seo, Changdae. Kim, J. Phys. Chem. Solids 67 (2006) 2316.
[14] D.-H. Cho, K. Hiraoa, K. Tanaka, N. Saga, J. Lumin. 68 (1996) 171.
[15] G. Park, T. Hayakawa, M. Nogami, J. Phys.: Condens. Matter 15 (2003) 1259.
[16] Qinghua Zeng, Zhiwu Pei, Shubing Wang, Qiang Su, Shaozhe Lu, Mater. Res. Bull. 34 (1999) 1837.
[17] Hongbin Liang, Qinghua Zeng, Tiandou Hu, Shubin Wang, Qiang Su, Solid State Sci. 5 (2003) 465.
[18] R. Stefani, A.D. Maia, E.E.S. Teotonio, M.A.F. Monteiro, M.C.F.C. Felinto, H.F. Brito, J. Solid State Chem. 179 (2006) 1086.
[19] Qinghua Zeng, Nathan Kilah, Mark Riley, J. Lumin. 101 (2003) 167.
[20] R. Kniep, G. Gozel, B. Eisenmann, C. Rohr, M. Asbrand, M. Kizilyalli, Angew. Chem. Int. Ed. Engl. 33 (1994) 749.
[21] A. Levesseur, R. Olazcuaga, M. Kbala, M. Zahir, P. Hagenmuller, M. Couzi, Solid State Ionics 9 (1981) 205.
[22] Y. Shi, J. Liang, H. Zhan, Q. Liu, X. Chen, J. Yang, W. Zhuang, G. Rao, J. Solid State Chem. 135 (1998) 43.
[23] H.Z. Bauer, Anorg. Allg. Chem. 345 (1966) 225.
[24] Y. Shi, J. Liang, J. Yang, W. Zhuang, G. Rao, J. Alloys Compds. 261 (1997) L1.
[25] G. Blasse, A. Bril, J. de Vries, J. Inorg. Nucl. Chem. 31 (1969) 568.
[26] S.L. Pan, Y.C. Wu, P.Z. Fu, G.C. Zhang, G.F. Wang, X.G. Guan, C.T. Chen, J. Cryst. Growth 236 (2002) 613.
[27] H. Song, T. Hayakawa, M. Nogami, J. Lumin. 81 (1999) 153.
[28] E.W.J.L. Oomen, A.M.A. van Dongen, J. Non-Cryst. Solids 111 (1989) 205.
[29] Weifeng. Li, Xigi. Feng, Chengjun. Duan, Jingtai. Zhao, Shili. Pan, Yicheng. Wu, J. Phys. D: Appl. Phys. 38 (2005) 385.
[30] B.V.R. Chowdari, G.V.S. Rao, C.J. Leo, Mater. Res. Bull. 36 (2001) 727.
[31] Shannon, Acta Crystallogr. A 32 (1976) 751.